RSC Advances

ROYAL SOCIETY OF CHEMISTRY

www.rsc.org/advances

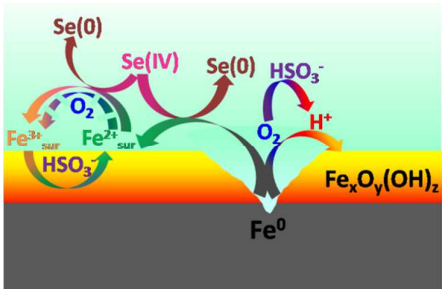

Graphical Abstract

The enhancing effect of HSO_3^- on Se(IV) sequestration varied with the headspace volume, HSO_3^- concentration and initial pH, respectively.

Enhancing Effect of Bisulfite on Sequestration of Selenite by Zerovalent Iron†

Jinxiang Li,[a‡] Chao Wang,[a‡] Junlian Qiao,*[a] Hejie Qin[ab] and Lina Li[b]

[a]State Key Laboratory of Pollution Control and Resources Reuse, College of Environmental Science and Engineering, Tongji University, Shanghai 200092, People's Republic of China

[b]Shanghai Synchrotron Radiation Facility, Shanghai Institute of Applied Physics, Chinese Academy of Sciences, Shanghai 201204, People's Republic of China

‡Authors contributed equally to this work.

†Electronic supplementary information (ESI) available.

E-mail addresses: ljx870616@126.com (J.X. Li), wangchao962@163.com (C. Wang), qiaoqiao@tongji.edu.cn (J.L. Qiao), chinhj@foxmail.com (H.J. Qin), lilina@sinap.ac.cn (L.N. Li)

*Author to whom correspondence should be addressed

Junlian Qiao, Email: qiaoqiao@tongji.edu.cn; Phone: +86-021-65489163

ABSTRACT

The enhancing effect of bisulfite (HSO_3^-) on the kinetics of Se(IV) sequestration by zerovalent iron (ZVI) was systematically investigated as functions of headspace volume, HSO_3^- concentration and initial pH (pH_{ini}). To exclude the role of HSO_3^- as an electrolyte, the kinetics of Se(IV) removal by ZVI with the presence of SO_4^{2-} was determined as a control. With increasing the headspace volume from 0 to 2.0 mL, the rate of Se(IV) removal by ZVI experienced a considerable enhancement whereas the further increase in the headspace volume resulted in a drop in Se(IV) removal rate. Se(IV) was always removed by ZVI with a higher rate in the presence of HSO_3^- than that in the presence of SO_4^{2-} at various headspace volume, which was mainly ascribed to the release of H^+ and the depletion of O_2 from the oxidation of HSO_3^- (i.e., $2HSO_3^- + O_2 \rightarrow 2SO_4^{2-} + 2H^+$). Furthermore, HSO_3^- accelerated the reduction of ferric oxides and hydroxides to Fe(II)-containing solid intermediate, which was beneficial to the reductive removal of Se(IV). The SEM, Fe *K*-edge XAFS and Se XANES analysis for Se(IV)-treated ZVI samples confirmed that HSO_3^- facilitated the transformation of ZVI to iron (oxyhydr)oxides (e.g., magnetite and lepidocrocite) and the reduction of Se(IV) to Se(0) compared to SO_4^{2-}. The enhancing effect of HSO_3^- on Se(IV) sequestration varied with the concentration of HSO_3^- and initial pH, with the greatest effect achieved at 2.0 mM of Se(IV) and pH_{ini} 5.0. Since bisulfite is inexpensive and its final product is sulfate, a common anion existing in water, taking advantage of bisulfite to enhance the ZVI's reactivity under limited oxygenated conditions is a promising method.

1. Introduction

Zerovalent iron (ZVI), as a readily available, inexpensive, nontoxic and moderately strong reducing agent,[1, 2] has been successfully applied for the remediation/treatment of groundwater/wastewater.[1, 3, 4] Nevertheless, owing to the inherent passive film, the granular ZVI or iron filings has low intrinsic reactivity towards contaminants in laboratory studies and field demonstrations.[1] Furthermore, the reactivity of ZVI decreased over time due to the precipitation of ferric (oxyhydr)oxides on the surface of iron.[5] Considering that the low reactivity of ZVI has become a major concern in the ZVI-based systems, it is highly desirable to develop methods that can significantly meliorate the reactivity of ZVI for its further environmental application.[1] Various countermeasures including acid washing,[6] H_2-reducing pretreatment,[7] combination with sonication[8] or weak magnetic field,[1, 4, 9] and electrochemical reduction,[10] as well as the synthesis of ZVI-based bimetals have been proposed to enhance the reactivity of ZVI.[11] Nevertheless, the disadvantages of these methods should be addressed, such as relatively complex procedures, extra costs, and ecotoxicity.[1, 2]

The inherent passive film and subsequent authigenic mineral precipitation are undesirable in environmental applications since they may mask the redox active sites where exchange of electrons between ZVI and contaminant or reduce the barrier permeability by occupying available pore space.[12] However, the Fe^{II} adsorbed to ferric oxides and hydroxides with higher reducing power (−0.35 to −0.65 V for $Fe_{(s)}^{III}/Fe_{(s)}^{II}$) than that of Fe^{II}/Fe^{0} (−0.44 V) has been reported to be beneficial for contaminants reduction.[13, 14] Recently, several studies have also confirmed that the Fe(II)-containing

solid intermediate, e.g., Fe(II)Fe(III) hydroxide,[13] green rust,[15, 16] magnetite,[17] and pyrite,[18] etc., can abiotically reduce contaminants whether the source of the Fe^{II} is bacteria-mediated regeneration,[19-21] chemical reduction,[22] or direct addition.[23, 24] Considering that the in situ generated Fe(III) can be rapidly reduced to Fe(II) by the inexpensive bisulfite (HSO_3^-) (Eq. (1)), taking advantage of bisulfite to enhance the ZVI's reactivity may be achieved. However, this hypothesis has not been validated. On one hand, oxygen (O_2) can be quenched by HSO_3^-, accompanied with the release of H^+ via Eq. (2).[25, 26] On the other hand, H^+ and O_2 had been reported to have great influence on the reactivity of ZVI toward contaminants.[1, 9, 27-29] Consequently, the coupled influence of HSO_3^- and O_2 on the reactivity of ZVI should be clarified.

$$HSO_3^- + 2Fe^{3+} + H_2O \rightarrow 2Fe^{2+} + SO_4^{2-} + 3H^+ \quad (1)$$

$$2HSO_3^- + O_2 \rightarrow 2SO_4^{2-} + 2H^+ \quad (2)$$

The prevalence of selenium in water poses a potential toxicity or deficiency to humans, animals, and some plants within a very narrow concentration range.[15, 30] Selenium-contaminated waters mainly originate from crude oil processing in refinery operations, discharging agricultural drainage and treating mining wastewater.[31, 32] Selenium can exist in aquatic environments in several states of oxidation: selenide (Se(-II)), selenium (Se(0)), selenite (Se(IV)), and selenate (Se(VI)).[33] The two oxidation states, Se(IV) and (Se(VI), are highly soluble, thus bioavailable and potentially toxic, while the reduced forms (Se(-II) and Se(0)) are insoluble and correspondingly much less bioavailable.[34] Moreover, the acute toxicity of Se(IV) is almost 10 times greater than that of Se(VI).[35] In view of the redox-dependent

solubility and toxicity of selenium, its oxyanions, particularly Se(IV), can precipitate as insoluble Se(0) or Se(-II) by reduction with ZVI or nanoscale ZVI,[3, 4, 36-39] thereby creating an efficient sink for selenium.[40, 41] Therefore, Se(IV) was employed as a target contaminant to examine the influence of HSO_3^- on the reactivity (i.e., the reductive capability) of ZVI.

In sum, the main objectives of this study were to (1) investigate the effect of HSO_3^- on the kinetics of Se(IV) sequestration by ZVI in limited oxygenated water; (2) determine the role of HSO_3^- in enhancing the reactivity of ZVI toward Se(IV) removal; (3) evaluate the effects of HSO_3^- concentration and initial solution pH on Se(IV) removal by ZVI under limited oxygenated conditions.

2. Experimental section

2.1. Materials.

All chemicals were of analytical grade and all solutions were prepared with Milli-Q water, unless otherwise specified. The ZVI used in this study was obtained from Sinopharm Chemical Reagent Co., Ltd., with a BET surface area of 0.15 $m^2 g^{-1}$. The SEM images, particle distribution and XRD pattern of the pristine ZVI sample employed in this study are presented in the Supporting Information (Fig. S1). All the other chemicals were purchased from Shanghai Qiangshun Chemical Reagent Company.

2.2. Bach Experiments.

To investigate the influence of HSO_3^- on the reactivity of ZVI toward Se(IV) removal in limited oxygenated water, the batch reactor experiments were performed in 25 mL

serum vials sealed with headspace containing air for 0-5.0 mL, which was injected by a syringe through the stopper. Prior to tests, reaction solution containing Se(IV) and background ions was freshly prepared by the N_2-sparged water in an anoxic chamber, then the initial pH was adjusted by dropwise addition of a NaOH or H_2SO_4 solution. No measure was taken to maintain the pH constant during the reaction. In a typical experiment, the dosage of ZVI was 2.0 mM and the initial concentration of Se(IV) was 10.0 mg L^{-1} while the concentration of HSO_3^- varied from 0 to 2.5 mM. Before being sealed and subsequent air injection to initiate an experimental run, the dosing of iron powder was immediately accomplished. The vials were sealed with the Teflon-lined butyl rubber stoppers and placed on a rolling mixer (60 rpm) in a temperature-controlled chamber (~25 ^oC). It should be specified that the bisulfite per se (without ZVI) could not remove Se(IV) (Fig. S2) and reduce Se(IV) to Se(0) since no pink color resulting from Se(0) was observed. Additionally, to exclude the role of HSO_3^- as an electrolyte and the influence of generated SO_4^{2-} on Se(IV) removal by ZVI, the experiments with SO_4^{2-} at same molar concentration as HSO_3^- were carried out to work as the control.

2.3. Chemical Analysis and Solid Phase Characterization.

The sample in each reaction vial was sacrificed for analysis, which was collected at given time intervals using a 10 mL syringe and filtered immediately through a 0.22 μm membrane filter, then acidified for analysis. Concentration of the residual selenium in the filtrate was analyzed using a PF5 atomic fluorescence spectrometer (Beijing Purkinje General Instrument Co., Ltd.) and the Fe(II) concentration in

131 solution was determined by the 1,10-phenanthroline colorimetric method using an
132 UV-visible spectrophotometer at 510 nm.[42]

133 Specific surface areas of the ZVI samples were determined by nitrogen adsorption
134 using the BET method (Micrometrics ASAP 2020). Morphology of the pristine ZVI
135 and the Se(IV)-treated ZVI samples was determined with Scanning Electron
136 Microscopy (SEM) using a Hitachi 4700 microscope. The size distribution of the
137 pristine ZVI particles was examined by a Bettersize 2000. The XRD pattern of the
138 pristine ZVI was collected using a Rigaku DXR-8000 computer-automated
139 diffractometer.

140 The reacted ZVI samples were collected on membrane filters (0.22 μm) and washed
141 with deionized water in a nitrogen-filled glove box, and then freeze-dried under
142 vacuum, and put them into zipper bags before being subjected to Fe *K*-edge and Se
143 *K*-edge X-Ray Absorption Fine Structure (XAFS) analysis. Particular care was taken
144 to minimize the beam-induced oxidation of samples by placing the sample stands
145 filled with reacted ZVI samples in a nitrogen-filled glove box for 6 hours before
146 transferring them to zippered bags in this glove box. Negligible changes in the
147 line-shape and peak position of Se *K*-edge X-ray absorption near edge structure
148 (XANES) spectra were observed between two scans taken for a specific sample. The
149 XAFS spectra were recorded at room temperature using a 4 channel Silicon Drift
150 Detector (SDD) Bruker 5040 at beam line BL14W1 of the Shanghai Synchrotron
151 Radiation Facility (SSRF), China. Fe and Se *K*-edge XAFS spectra were recorded in
152 transmission mode and fluorescence mode using a Si(111) double crystal

monochromator, respectively. The spectra were processed and analyzed by the software codes Athena.[43] The oxidation states of selenium in solid phase were analyzed by linear combination fitting (LCF) using reference compounds of FeSe (Se(-II)), Se powder (Se(0)), Na_2SeO_3 (Se(IV)) and Na_2SeO_4 (Se(VI)). The major species of Fe in Se-treated ZVI corrosion products were also quantified by LCF using the collection of reference materials including metallic Fe (Fe^0), wustite (FeO), maghemite (γ-Fe_2O_3), magnetite (Fe_3O_4), goethite (α-FeOOH) and lepidocrocite (γ-FeOOH).

3. Results and discussion

3.1. Oxygen Effect on the Reactivity of ZVI toward Se(IV) Sequestration.

The influence of headspace volume on the kinetics of Se(IV) removal by ZVI was investigated, as depicted in Fig. 1. Obviously, headspace remarkably improved the reactivity of ZVI toward substrate regardless the presence of SO_4^{2-} or HSO_3^-. Approximately 34.8%-94.8% of Se(IV) was removed by ZVI in 180 min in limited oxygenated water (V_{air} = 0.5-5.0 mL), whereas only 10.7%-28.9% of Se(IV) was sequestrated by ZVI within the same period but under anoxic condition. The O_2-dependent characteristic of the ZVI's reactivity toward contaminants had also been reported by other researchers and was always explained by the promoted ZVI dissolution rate (Eqs. (3) and (4)) and/or the formation of the Fe(II)-solid intermediate and Fe(III) (oxyhydr)oxides on the ZVI surface providing reducing power and large surface area.[13, 27, 44-46]

$$2Fe^0 + O_2 + 2H_2O \rightarrow 2Fe^{2+} + 4OH^- \quad (3)$$

$$2Fe^0 + O_2 + 4H^+ \rightarrow 2Fe^{2+} + 2H_2O \quad (4)$$

3.2. Coupled Effects of O_2 and HSO_3^- on the Reactivity of ZVI toward Se(IV) Sequestration.

As illustrated in Fig. 1, a brief lag phase appeared in the kinetics of Se(IV) removal by ZVI in the presence of SO_4^{2-} or HSO_3^-, both in this study and in our previous work.[1, 3, 4, 9, 36] Analogous effects have been reported in previous investigations with a diversity of iron types and contaminant natures.[4, 47, 48]

In the presence of SO_4^{2-}, it was found that the lag period of Se(IV) removal by ZVI was gradually alleviated from 60 to 20 min with increasing the volume of headspace from 0.5 to 5.0 mL. The lag behavior in the initial period of Se(IV) removal by ZVI was mainly ascribed to the oxide film coated on the pristine ZVI particles inhibiting the mass transfer of substrate to the Fe^0 surface.[9] The other possible explanation for this transient behavior was that the O_2 in headspace, which expedites the pitting of the passive film (Eqs.(3)-(6)), and thus, Se(IV) reduction by ZVI via Eq. (7).

$$Fe^0 + 2H_2O \rightarrow Fe^{2+} + H_2 + 2OH^- \quad (5)$$

$$Fe^0 + 2H^+ \rightarrow Fe^{2+} + H_2 \quad (6)$$

$$2Fe^0 + HSeO_3^- + 5H^+ \rightarrow 2Fe^{2+} + Se^0 \downarrow + 3H_2O \quad (7)$$

After the lag period, the main portion of each data set can be reasonably well simulated by the pseudo-first-order rate law (Eq. (8)).[49]

$$\frac{\mathrm{d}[Se(IV)]}{\mathrm{dt}} = -k_{\mathrm{obs}}[Se(IV)] \quad (8)$$

where k_{obs} is the observed pseudo-first-order rate constant (min^{-1}) for Se(IV) removal by ZVI. As demonstrated by in Fig. 1 and Fig. S3, a 4-fold enhancement,

from 0.0008 to 0.0031-0.0037 min^{-1}, was observed in the rate constants of Se(IV) disappearance by increasing the headspace volume from 0 to 5 mL. Nevertheless, increasing the volume of headspace from 0.5 mL to 5.0 mL had minor effect on the reactivity of ZVI toward Se(IV) removal, indicating that O_2 (i.e., V_{air} > 0.5 mL) was no longer involved in the rate controlling step for Se(IV) removal by ZVI in the presence of SO_4^{2-}.

As for the kinetics of Se(IV) removal by ZVI in the presence of HSO_3^-, the lag behavior was susceptible to the headspace volume and the lag phase shortened from 20 to 0 min with increasing the volume of headspace from 0.5 to 5.0 mL. In addition, Figs. 1 and S4 revealed that the performances of ZVI for Se(IV) sequestration experienced a more dynamic and more variable scenario compared to that in the coexistence of headspace and SO_4^{2-}, accompanied with a distinctively bell-shaped pattern associated with the headspace space. The Se(IV) sequestration rate constant was enhanced progressively from 0.0016 to 0.0292 min^{-1} with increasing the headspace for containing air from 0 to 2.0 mL. With further increase in the headspace volume, the reactivity of ZVI reached a relatively recession. It should be emphasized that the ZVI remained a higher performance for removing Se(IV) in oxygenated water than that without headspace, which should be largely associated with the reduction of Fe(III) (oxyhydr)oxides to the Fe(II)-solid intermediate by HSO_3^- on the ZVI surface providing reducing power for Se(IV) following Eqs. (7) and (9).[50, 51]

$$4Fe^{2+} + HSeO_3^- + 9H_2O \rightarrow 4Fe(OH)_3 + Se^0 \downarrow + 7H^+ \quad (9)$$

Fig. 1 demonstrates that the coupled effects of O_2 and HSO_3^- resulted in faster

selenium removal kinetics than that in the coexistence of O_2 and SO_4^{2-}, which were consistent with the variations of aqueous Fe(II) concentrations and solution pH during Se(IV) sequestration by ZVI in the presence of SO_4^{2-}/HSO_3^- and O_2, as shown in Fig. 2.

In the presence of SO_4^{2-}, the concentration of Fe(II) increased progressively within 45 min and then dropped gradually in the process of Se(IV) removal by ZVI, which was accompanied with a mild increase of solution pH during the initial stage of reaction. Hereafter, pH was almost constant, which may be associated with the Fe^{2+} oxidation by O_2 and Fe^{3+} hydrolysis (Eqs. 10-11). Different from the case in the presence of SO_4^{2-}, the solution pH during Se(IV) removal by ZVI in the presence of HSO_3^- dropped dramatically during the initial period of reaction (from 0 to 10.0 or 30 min, Eq. (2)) and hereafter experienced a progressively elevated stage, accompanied with a rapid release of Fe(II) with prolonged reaction time. Moreover, Fe(III) can be reduced to Fe(II) by HSO_3^- via Eq. (1), accompanied with the release SO_4^{2-} and H^+, which favors the corrosion of ZVI, accounting for the trend in the release of Fe(II).

$$4Fe^{2+} + O_2 + 2H_2O \rightarrow 4Fe^{3+} + 4OH^- \quad (10)$$

$$Fe^{3+} + 3H_2O \rightarrow 2Fe(OH)_3 + 3H^+ \quad (11)$$

3.3. Iron Corrosion and Selenium Speciation Transformation in Se(IV)-treated ZVI Samples.

The ZVI corrosion behaviors with presence of O_2 and HSO_3^- were further clarified by characterizing the Se(IV)-treated ZVI samples. The pristine ZVI used in this study was consisted of relatively smooth spheres (Fig. S1 (a)) and became slightly coarse

during reacted with Se(IV) in the presence of SO_4^{2-} for 30 min, 60 min and 180 min, respectively (Fig. S5). Comparably, the Se(IV)-treated ZVI particles in the presence of HSO_3^- became more cracked with angular-shaped and platy structures (Fig. S5), implying the more extensive corrosion upon the introduction of HSO_3^-. Moreover, the Fe *K*-edge XANES spectra and k^3-weighted EXAFS spectra of these two Se(IV)-treated ZVI samples and the reference materials were shown in Fig. 3(a-b). In the presence of SO_4^{2-}, the XANES and EXAFS spectra of Se(IV)-treated ZVI sample was more analogous to that of the Fe^0 than that with the presence of HSO_3^- (Fig. 3(a)). Meanwhile, the latter sample was more analogous to those of the Fe(II)/Fe(III) reference compounds (Fig. 3(a)), implying that these solids were mainly composed of nonmetallic Fe. To identify the composition of corrosion products, linear combination fitting (LCF) analysis was carried out based on the Fe k^3-weighted EXAFS spectra (Fig. 3(b)) and the corresponding fit results were summarized in Table. S1. In the presence of SO_4^{2-}, the Se(IV)-treated ZVI sample was consist of magnetite (43.0%), wustite (20.4%), ferrihydrite (9.5%), lepidocrocite (8.0%), and some metallic Fe^0 (19.1%). hen SO_4^{2-} was replaced with HSO_3^-, the fraction of Fe^0 in the Se(IV)-treated ZVI sample decreased greatly to 5.4% and ZVI corrosion was considerably enhanced with the major corrosion products being magnetite (57.7%) and lepidocrocite (19.4%), along with some wustite (8.2%) and maghemite (9.3%). It was generally acknowledged that the very high conductivity of magnetite with almost metallic character was beneficial for the electron transport and the loose and porous structure of lepidocrocite favored the mass transport between the solid phase and aqueous

254 phase.[52, 53] Therefore, it could be inferred that the appreciable reactivity of ZVI was
255 mainly associated with the involvement of magnetite and lepidocrocite.

256 To further explore the coupled effects of O_2-HSO_3^- on the reactivity of ZVI
257 toward Se(IV) removal, the selenium speciation in the corresponded precipitates
258 collected at 180 min was analyzed with XANES, as demonstrated in Fig. 3(c). The Se
259 *K*-edge XANES data for several Se reference compounds including FeSe (Se(-II)),
260 selenium powder (Se(0)), sodium selenite (Se(IV)), and sodium selenate (Se(VI))
261 were analyzed to establish the reference X-ray absorption *K*-edge energies (E_0).[46, 54]
262 The XANES spectrum of Se(IV)-treated ZVI in the presence of O_2 and HSO_3^-
263 demonstrated that Se(IV) removal by ZVI was mainly achieved via reduction
264 following Eqs. (7) and (9). However, only partial of the removed Se(IV) was reduced
265 to Se(0) when SO_4^{2-} was employed as background electrolyte. The transient Se(IV)
266 adsorption step on the reductive surface forming the shell surrounding the iron core
267 should be necessary for reduction of dissolved Se(IV) by ZVI and adsorbed Fe(II).[1, 3,
268 55] Therefore, it could be concluded that the coupled presence of O_2 and HSO_3^- was
269 more beneficial for the reduction of Se(IV) to Se(0) as compared to that by the
270 synergetic effects of O_2 and SO_4^{2-}.

271 **3.4. Effects of SO_4^{2-}/HSO_3^- Concentration and pH on Se(IV) Sequestration by**
272 **ZVI.**

273 The influence of SO_4^{2-}/HSO_3^- concentrations on the kinetics of Se(IV) sequestration
274 by ZVI in limited oxygenated water at pH_{ini} 5.0 were demonstrated in Fig. 4. At
275 various SO_4^{2-}/HSO_3^- concentrations, ZVI always removed Se(IV) at higher rate

constants in the presence of HSO_3^- than those in the presence of SO_4^{2-}. In addition, the kinetics of selenium disappearance could be roughly divided into two stages, a lag period followed by a rapid removal period, which was simulated with pseudo-first order model (Eq. (8)). It was found that the rate constants of Se(IV) removal by ZVI were increased appreciably from 0.0008 to 0.0059 min^{-1} whereas did not mediate the lag period with increasing the concentration of SO_4^{2-} from 0 to 2.5 mM, implying that the iron oxides coated on the pristine ZVI particles could weaken the enhancement for Se(IV) removal by SO_4^{2-}. On the contrary, after the introduction of HSO_3^-, the lag phase in the initial period of Se(IV) removal by ZVI was shortened from 20 to 10 min with increasing the HSO_3^- concentration from 0.5 to 2.5 mM. Moreover, the rate constants of Se(IV) sequestration by ZVI were enhanced progressively from 0.0079 to 0.0292 min^{-1} as the concentration of HSO_3^- was elevated from 0.5 to 2.0 mM. However, as the concentration of HSO_3^- was further increased to 2.5 mM, the removal rate of Se(IV) decreased to 0.0144 min^{-1}. The influence of HSO_3^- concentration on the reactivity of ZVI should be mainly associated with the H^+ release and the O_2 depletion from the oxidation of HSO_3^- following Eq. (2). With increasing the HSO_3^- concentration, the progressive enhancements should be likely due to the decline of solution pH and the depletion of O_2 preventing the passivation of ZVI. However, HSO_3^- of high concentration will quench O_2, which will inhibit the formation of the Fe(III) (oxyhydr)oxides co-precipitating with Se(IV) and the galvanic corrosion of ZVI, and thus, Se(IV) reduction by ZVI via Eq. (7).

The effects of SO_4^{2-}/HSO_3^- on Se(IV) removal by ZVI in limited oxygenated water

over the pH_{ini} of 3.0-7.0 were also evaluated, as depicted in Fig. 5. $HSeO_3^-$ is the major specie of the aqueous Se(IV) at pH 3.0-7.0 since the pK_{a1} and pK_{a2} of H_2SeO_3 are 2.62 and 8.23, respectively (Fig. S6).[56] Thus, the synergetic effects of O_2 and pH_{ini} on Se(IV) removal should be rarely ascribed to the species variation of Se(IV).[1] Regardless the introduction of SO_4^{2-} or HSO_3^-, the removal of Se(IV) by ZVI exhibited self-acceleration characteristics, which involved a lag period and hereafter a rapid removal period. The duration of lag period extended gradually with increasing the pH_{ini}, verifying that the lower pH facilitated the abrasion of passive iron oxide layer and thus shortened the lag period.[1, 2, 9] Beyond the lag period, it was additionally found that the pseudo-first-order rate constants (k_{obs}) for Se(IV) removal in the presence of SO_4^{2-} were dampen dramatically from 0.0084 to 0.0014 min^{-1} with increasing the solution pH_{ini}. Alternatively, the introduction of HSO_3^- markedly accelerated Se(IV) removal by ZVI and the k_{obs} were 0.0168, 0.0116, 0.0292, 0.0128 and 0.0073 min^{-1} at pH_{ini} 3.0, 4.0, 5.0, 6.0 and 7.0, respectively. The best performance of ZVI for Se(IV) removal in the presence of HSO_3^- was achieved at pH_{ini} 5.0. It was well known that the adsorbed Fe(II) on ZVI surface contributed to the reductive removal of Se(IV).[3] With increasing pH_{ini}, the reductive ability of Fe(II) increased while the amount of released Fe(II) dropped (Fig. S7),[57] and thus the most efficient Se(IV) removal was observed at pH_{ini} 5.0.

4. Conclusions

The bisulfite induced a significant enhancement on the kinetics of Se(IV) removal by ZVI and the improvement should be mainly ascribed to the release of H^+ and the

depletion of O_2 arising from the oxidation of HSO_3^-. In addition, HSO_3^- facilitated the reduction of ferric (oxyhydr)oxides to Fe(II)-containing solid, which was beneficial to the reductive removal of Se(IV). Over the HSO_3^- concentration of 0-2.5 mM or pH_{ini} range of 3.0-7.0, ZVI could always keep higher reactivity toward Se(IV) sequestration in the presence of HSO_3^- than that in the presence of SO_4^{2-}. The coupled effects of O_2 and HSO_3^- on ZVI's reactivity toward Se(IV) removal experienced a more dynamic and more variable scenario (bell-shaped) than that in the presence of O_2 and SO_4^{2-}. Furthermore, the SEM, Fe *K*-edge XAFS and Se XANES analysis for Se(IV)-treated ZVI samples unraveled that binding O_2 and HSO_3^- favored the transformation of ZVI to iron (oxyhydr)oxides (e.g., magnetite and lepidocrocite) and the reduction of Se(IV) to Se(0). Compared to the previous strategies for maintaining or enhancing the reactivity of ZVI, applying bisulfite will provide a promising alternative to improve the performance of the ZVI-based technology for environmental application, since the bisulfite is efficient, inexpensive and its final product is harmless. However, more efforts should be taken to evaluate this technology more thoroughly on field-scale abatement practices.

Acknowledgements

This work was supported by the youth project of National Natural Science Fund (Grant 11405256) and Shanghai Municipal Natural Science Foundation (Grant 13ZR1447800). The authors thank the beamline BL14W1 (Shanghai Synchrotron Radiation Facility) for providing the beam time.

References

1. L. Liang, W. Sun, X. Guan, Y. Huang, W. Choi, H. Bao, L. Li and Z. Jiang, *Water Res.*, 2014, **49**, 371-380.

2. X. Guan, Y. Sun, H. Qin, J. Li, I. M. Lo, D. He and H. Dong, *Water Res.*, 2015, **75**, 224-248.

3. L. Liang, W. Yang, X. Guan, J. Li, Z. Xu, J. Wu, Y. Huang and X. Zhang, *Water Res.*, 2013, **47**, 5846-5855.

4. L. P. Liang, X. H. Guan, Z. Shi, J. L. Li, Y. N. Wu and P. G. Tratnyek, *Environ. Sci. Technol.*, 2014, **48**, 6326-6334.

5. C. B. Wang and W. X. Zhang, *Environ. Sci. Technol.*, 1997, **31**, 2154-2156.

6. K. C. K. Lai and I. M. C. Lo, *Environ. Sci. Technol.*, 2008, **42**, 1238-1244.

7. Y. H. Liou, S. L. Lo, C. J. Lin, W. H. Kuan and S. C. Weng, *J. Hazard. Mater.*, 2005, **126**, 189-194.

8. C. L. Geiger, C. A. Clausen, D. R. Reinhart, C. M. Clausen, N. Ruiz and J. Quinn, *Acs. Sym. Ser.*, 2003, **837**, 286-303.

9. Y. K. Sun, X. H. Guan, J. M. Wang, X. G. Meng, C. H. Xu and G. M. Zhou, *Environ. Sci. Technol.*, 2014, **48**, 6850-6858.

10. L. Chen, S. Jin, P. H. Fallgren, N. G. Swoboda-Colberg, F. Liu and P. J. S. Colberg, *J. Hazard. Mater.*, 2012, **239**, 265-269.

11. B. W. Zhu and T. T. Lim, *Environ. Sci. Technol.*, 2007, **41**, 7523-7529.

12. Y. Furukawa, J.-w. Kim, J. Watkins and R. T. Wilkin, *Environ. Sci. Technol.*, 2002, **36**, 5469-5475.

13. A. C. Scheinost and L. Charlet, *Environ. Sci. Technol.*, 2008, **42**, 1984-1989.

14. A. F. White and M. L. Peterson, *Geochim. Cosmochim. Ac.*, 1996, **60**, 3799-3814.

15. S. C. B. Myneni, T. K. Tokunaga and G. E. Brown, *Science*, 1997, **278**, 1106-1109.

16. A. M. Scheidegger, D. Grolimund, D. Cui, J. Devoy, K. Spahiu, P. Wersin, I. Bonhoure and M. Janousch, *J. Phys. Iv.*, 2003, **104**, 417-420.

17. C. A. Gorski, J. T. Nurmi, P. G. Tratnyek, T. B. Hofstetter and M. M. Scherer, *Environ. Sci. Technol.*, 2010, **44**, 55-60.

18. C. Bruggeman, A. Maes, J. Vancluysen and P. Vandenmussele, *Environ. Pollut.*, 2005, **137**, 209-221.

19. M. L. McCormick, E. J. Bouwer and P. Adriaens, *Environ. Sci. Technol.*, 2002, **36**, 403-410.

20. H. Y. Shin, N. Singhal and J. W. Park, *Chemosphere*, 2007, **68**, 1129-1134.

21. B. Lai, Y. X. Zhou, P. Yang, J. L. Wang, J. H. Yang and H. Q. Li, *J. Hazard. Mater.*, 2012, **241**, 241-251.

22. S. Kim and F. W. Picardal, *Environ. Toxicol. Chem.*, 1999, **18**, 2142-2150.

23. R. A. Maithreepala and R. A. Doong, *Environ. Sci. Technol.*, 2004, **38**, 260-268.

24. J. E. Amonette, D. J. Workman, D. W. Kennedy, J. S. Fruchter and Y. A. Gorby, *Environ. Sci. Technol.*, 2000, **34**, 4606-4613.

25. R. E. Connick, Y. X. Zhang, S. Y. Lee, R. Adamic and P. Chieng, *Inorg. Chem.*, 1995, **34**, 4543-4553.

26. R. E. Connick and Y. X. Zhang, *Inorg. Chem.*, 1996, **35**, 4613-4621.

27. L. F. Greenlee, J. D. Torrey, R. L. Amaro and J. M. Shaw, *Environ. Sci. Technol.*,

2012, **46**, 12913-12920.

28. P. Sarin, V. L. Snoeyink, J. Bebee, K. K. Jim, M. A. Beckett, W. M. Kriven and J. A. Clement, *Water Res.*, 2004, **38**, 1259-1269.

29. B. Gu, T. J. Phelps, L. Liang, M. J. Dickey, Y. Roh, B. L. Kinsall, A. V. Palumbo and G. K. Jacobs, *Environ. Sci. Technol.*, 1999, **33**, 2170-2177.

30. B. D. Gibson, D. W. Blowes, M. B. J. Lindsay and C. J. Ptacek, *J. Hazard. Mater.*, 2012, **241**, 92-100.

31. Y. Q. Zhang and J. N. Moore, *Environ. Sci. Technol.*, 1996, **30**, 2613-2619.

32. X. G. Meng, S. Bang and G. P. Korfiatis, *Water Res.*, 2002, **36**, 3867-3873.

33. C. V. Putnis, F. Renard, H. E. King, G. Montes-Hernandez and E. Ruiz-Agudo, *Environ. Sci. Technol.*, 2013, **47**, 13469-13476.

34. Y. Q. Zhang, C. Amrhein, A. Chang and W. T. Frankenberger, *Sci. Total. Environ.*, 2008, **407**, 89-96.

35. R. L. D. Loyo, S. I. Nikitenko, A. C. Scheinost and M. Simonoff, *Environ. Sci. Technol.*, 2008, **42**, 2451-2456.

36. L. P. Liang, X. Jiang, W. J. Yang, Y. Y. Huang, X. H. Guan and L. N. Li, *Desalin. Water Treat.*, 2015, **53**, 2540-2548.

37. R. Liu and R. Lal, *J. Nanotechnol.*, 2012, **2012**, 1-18.

38. R. A. Crane and T. B. Scott, *J. Hazard. Mater.*, 2012, **211**, 112-125.

39. L. Ling, B. C. Pan and W. X. Zhang, *Water Res.*, 2015, **71**, 274-281.

40. T. K. Tokunaga, G. E. Brown, I. J. Pickering, S. R. Sutton and S. Bait, *Environ. Sci. Technol.*, 1997, **31**, 1419-1425.

41. Y. Q. Zhang and J. N. Moore, *Appl. Geochem.*, 1997, **12**, 685-691.

42. Y. K. Sun, X. M. Xiong, G. M. Zhou, C. Y. Li and X. H. Guan, *Sep. Purif. Technol.*, 2013, **115**, 198-204.

43. B. Ravel and M. Newville, *J. Synchrotron Radiat*, 2005, **12**, 537-541.

44. S. Klas and D. W. Kirk, *Sep. Purif. Technol.*, 2013, **116**, 222-229.

45. S. Klas and D. W. Kirk, *J. Hazard. Mater.*, 2013, **252**, 77-82.

46. I. H. Yoon, K. W. Kim, S. Bang and M. G. Kim, *Appl. Catal. B-Environ.*, 2011, **104**, 185-192.

47. X. Jiang, J. Qiao, I. M. C. Lo, L. Wang, X. Guan, Z. Lu, G. Zhou and C. Xu, *J. Hazard. Mater.*, 2015, **283**, 880-887.

48. R. Miehr, P. G. Tratnyek, J. Z. Bandstra, M. M. Scherer, M. J. Alowitz and E. J. Bylaska, *Environ. Sci. Technol.*, 2004, **38**, 139-147.

49. T. L. Johnson, M. M. Scherer and P. G. Tratnyek, *Environ. Sci. Technol.*, 1996, **30**, 2634-2640.

50. L. Xie and C. Shang, *Chemosphere*, 2007, **66**, 1652-1659.

51. P. Westerhoff and J. James, *Water Res.*, 2003, **37**, 1818-1830.

52. F. D. Coelho, J. D. Ardisson, F. C. C. Moura, R. M. Lago, E. Murad and J. D. Fabris, *Chemosphere*, 2008, **71**, 90-96.

53. A. Neumann, R. Kaegi, A. Voegelin, A. Hussam, A. K. M. Munir and S. J. Hug, *Environ. Sci. Technol.*, 2013, **47**, 4544-4554.

54. J. T. Olegario, N. Yee, M. Miller, J. Sczepaniak and B. Manning, *J. Nanopart. Res.*, 2010, **12**, 2057-2068.

55. Y. Q. Zhang, J. F. Wang, C. Amrhein and W. T. Frankenberger, *J. Environ. Qual.*, 2005, **34**, 487-495.

56. T. Z. Su, X. H. Guan, G. W. Gu and J. M. Wang, *J. Colloid Interf. Sci.*, 2008, **326**, 347-353.

57. X. H. Guan, H. R. Dong, J. Ma, I. M. C. Lo and X. M. Dou, *Sep. Purif. Technol.*, 2011, **80**, 179-185.

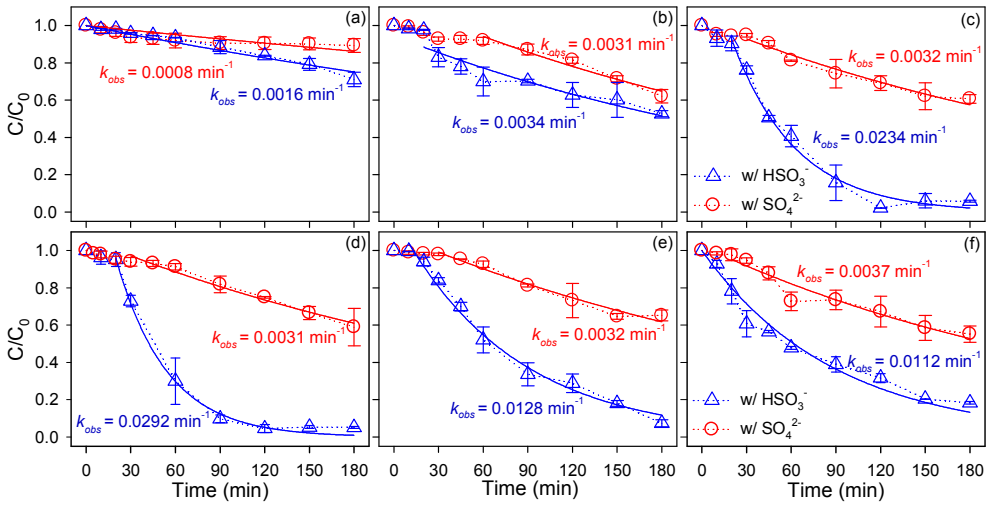

436

437 **Figure 1.** The kinetics of Se(IV) removal by ZVI in glass vials sealed with headspace

438 containing air (V_{air}) for 0 (a), 0.5 (b), 1.0 (c), 2.0 (d), 3.0 (e) and 5.0 mL (f),

439 respectively. The solid lines are the results of simulating the kinetics with

440 pseudo-first-order model. Reaction conditions: $[Fe^0]$ = 2.0 mM, $[Se(IV)]_0$ = 10.0 mg

441 L^{-1}, $[SO_4^{2-}/HSO_3^-]_0$ = 2.0 mM, pH_{ini} = 5.0.

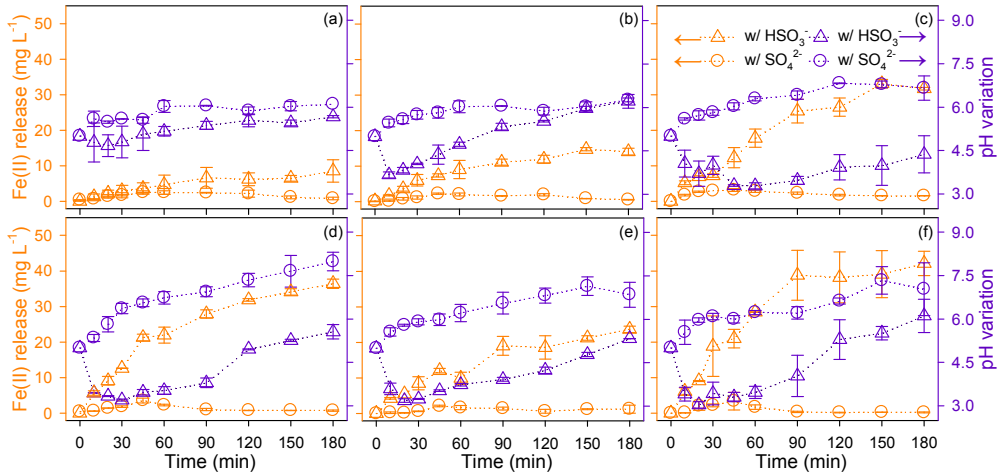

442

443 **Figure 2.** Variations in dissolved Fe(II) and pH during Se(IV) removal by ZVI in

444 glass vial sealed with the Teflon-lined butyl rubber stoppers containing containing air

445 (V_{air}) for 0 (a), 0.5 (b), 1.0 (c), 2.0 (d), 3.0 (e) and 5.0 mL (f), respectively.

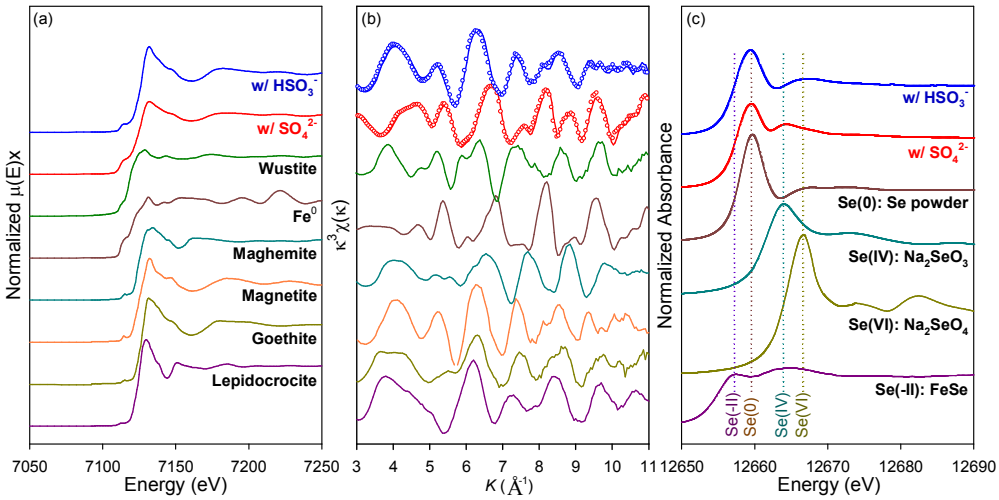

Figure 3. Fe *K*-edge XANES spectra (a), Fe k^3-weighted EXAFS spectra (b) and Se *K*-edge XANES spectra (c) of the Se(IV)-treated ZVI corrosion products at 180 min, as well as the corresponding reference materials. The circles and the thick solid lines (b) represent the linear combination fits and the experimental data, respectively. Reaction conditions: $[Fe^0] = 2.0$ mM, $[Se(IV)]_0 = 10.0$ mg L^{-1}, $[SO_4^{2-}/HSO_3^-]_0 = 2.0$ mM, $pH_{ini} = 5.0$, $V_{air} = 2.0$ mL.

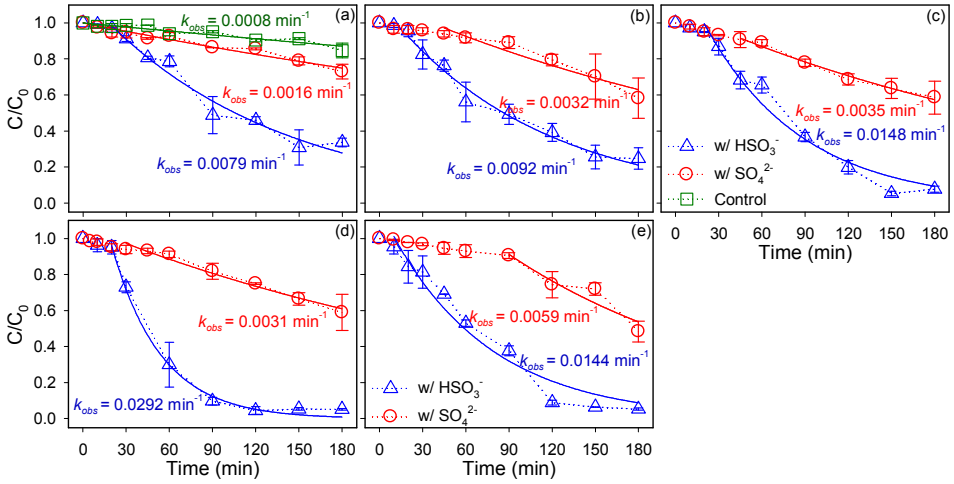

453

454 **Figure 4.** The kinetics of Se(IV) removal by ZVI with the presence of SO_4^{2-} or HSO_3^-

455 for 0 mM ((a): Control), 0.5 (a), 1.0 (b), 1.5 (c), 2.0 (d) and 2.5 mM (e), respectively.

456 The solid lines are the results of simulating the kinetics with pseudo-first-order model.

457 Reaction conditions: $[Fe^0] = 2.0$ mM, $[Se(IV)]_0 = 10.0$ mg L^{-1}, $[pH]_{ini} = 5.0$, $V_{air} = 2.0$

458 mL.

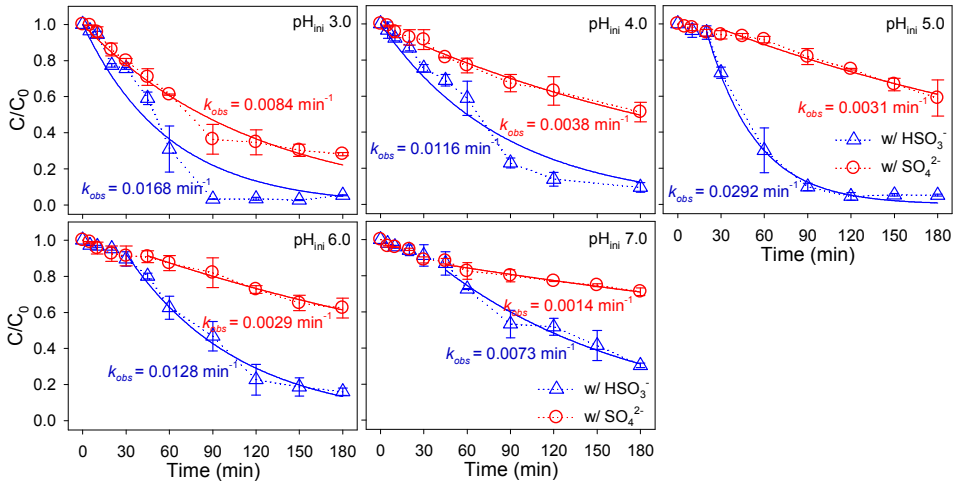

459

460 **Figure 5.** The kinetics of Se(IV) removal by ZVI at various pH_{ini} levels. The solid

461 lines are the results of simulating the kinetics with pseudo-first-order model. Reaction

462 conditions: $[Fe^0] = 2.0$ mM, $[Se(IV)]_0 = 10.0$ mg L^{-1}, $[HSO_3^-/SO_4^{2-}]_0 = 2.0$ mM, V_{air} =

463 2.0 mL.